

# DOSIMETRY ANALYSIS OF BORON NEUTRON CAPTURE THERAPY (BNCT) ON THYROID CANCER USING PHITS CODE WITH NEUTRON FROM 30 MeV CYCLOTRON

Bilalodin Bilalodin\*, Wihantoro, Aris Haryadi, Farzand Abdullatif

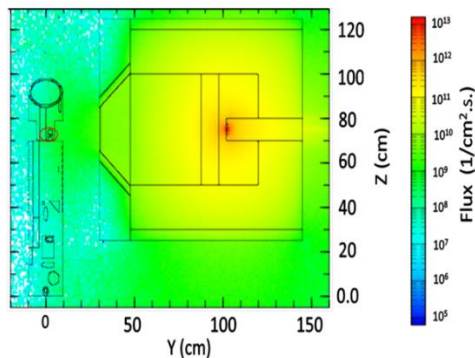
Department of Physics, Faculty Mathematics and natural Science,  
Jenderal Soedirman University, Indonesia

## Article history

Received  
1 November 2022  
Received in revised form  
18 May 2023  
Accepted  
11 June 2023  
Published Online  
21 August 2023

\*Corresponding author  
bilalodin@unsoed.ac.id

## Graphical abstract



## Abstract

The dosimetry analysis of Boron Neutron Capture Therapy (BNCT) on thyroid cancer using the Particle and Heavy Ion Transport Code System (PHITS) has been carried out. The purpose of research was to determine the received dose rate and the irradiation time required for thyroid cancer therapy using the BNCT method. The geometry of thyroid model is based on MIRD phantom with cancer cells located in the center of the thyroid. The phantom was irradiated using a neutron source from DLBSA based 30 MeV cyclotron. Simulations were carried out at boron concentrations of (10, 20, 30, 40, 50, 60, and 70)  $\mu\text{g/g}$  tissue. Simulation results show that the boron concentration increases with dose rate. The highest dose rate was obtained in the Gross Target Volume (GTV) of  $1.590 \times 10^{-2}$  Gy/s using a boron concentration of 70 mg/g tissue. The effective time for cancer therapy was calculated based on the highest dose rate obtained at 57 minutes.

Keywords: Dosimetry, BNCT, thyroid cancer, cyclotron, PHITS

© 2023 Penerbit UTM Press. All rights reserved

## 1.0 INTRODUCTION

The thyroid gland is one of the largest endocrine glands in the human body. Its main function is to provide adequate thyroid hormone for regulating body functions such as energy expenditure and metabolism [1]. The thyroid gland is located in the front of the neck. The upper part is connected to the larynx and the lower part to the trachea. The thyroid gland shapes like a butterfly, consisting of right and left lobes [2]. Thyroid gland cancer can arise as a lump at the bottom or side of the Adam's apple [3].

Thyroid cancer can be treated using internal and external therapy. Internal therapy typically uses iodine 131 radioactive fluid, while external therapy uses radiotherapy. In general, the total dose required for thyroid cancer therapy using radiotherapy is 54 Gy and given in increments of 1.5 Gy each time [4].

The weakness of the radiotherapy method is that it risks other organs around the thyroid gland from receiving large doses of radiation, resulting in damage to these organs [5]. Besides, it takes a long time to reach the total dose; within reasonable therapy time, the population of cancer cells decreases but is not eliminated [6]. Therefore, more effective methods that can minimize these weaknesses are needed. Such methods include the Boron Neutron Capture Therapy (BNCT) method, which has been licensed for cancer therapy, especially for cancer that infects the head and neck organs [7].

The working principle of BNCT is shown in Figure 1. The interaction between a  $^{10}\text{B}$  and a thermal neutron forms excited state B-11. The B-11 will split into an alpha particle and a lithium nucleus with release of energy. The decay of the  $^{11}\text{B}$  isotope can occur in

two mechanisms. The first mechanism, with a probability of 6.1%, produces an alpha particle and a lithium nucleus releasing energy of 2.79 MeV. The second one, with a probability of 93.9%, produces an alpha particle and a lithium nucleus with an energy release of 2.31 MeV. The unstable lithium core emits gamma radiation with energy of 0.48 MeV. Both reaction mechanisms are shown in Figure 1 [8].

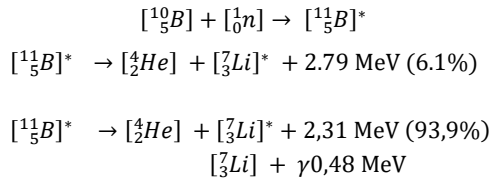


**Figure 1** Reaction mechanism of neutron thermal with boron-10 ( $^{10}\text{B}$ )

The success of any therapy with the BNCT method depends on two things, namely the ability of  $^{10}\text{B}$  to accumulate in cancer cells and the availability of a neutron source capable of reaching  $^{10}\text{B}$  in these cancer cells [9]. The neutron source currently being developed comes from accelerators. One form of accelerator developed is the 30 MeV cyclotron. Cyclotrons equipped with the Beam Shaping Assembly (BSA) system are capable of producing epithermal neutrons with energies between  $10^{-6}$  to  $10^{-2}$  MeV [8]. Epithermal neutrons have a deeper reach in body tissues [10, 11]. Therefore, the neutron source of the 30 MeV cyclotron is considered suitable for the treatment of cancers such as thyroid cancer.

It is necessary to calculate the correct dose before any cancer therapy. The concentration of  $^{10}\text{B}$  needs to be determined precisely to provide the maximum dose. The four components of the BNCT dose that need to be determined are boron dose, gamma dose, proton dose, and neutron dose. A software for calculating the dose in BNCT is the Particle and Heavy Ion Transport code System (PHITS). The PHITS is a Monte Carlo-based software developed by the Japan Atomic Energy Agency (JAEA) and the JAERI Computational Dosimetry System (JCDS) [12]. It can be used to evaluate the dose or dose rate absorbed by each organ and visualize the traces of particles passing through that organ [13]. This article will describe the results of dose analysis in thyroid cancer using the PHITS code with a neutron source derived from a 30 MeV cyclotron-based Double Layer Beam Shaping Assembly (DLBSA).

## 2.0 METHODOLOGY

### 2.1 Neck Phantom and Neutron Source

The neck phantom model refers to the MIRD phantom model [14]. It consists of skin tissue, muscle, thyroid gland, and neck bone (spine). The skin,

muscle, and spine tissues are cylindrical in shape, with diameters of 10.8 cm, 10.4 cm, and 3 cm, respectively. Cancer cells are in the form of a ball 1 cm in diameter located in the right thyroid gland at a depth of 2.4 cm. The cancer tissue is divided into three parts, namely Gross Target Volume (GTV), Clinical Target Volume (CTV), and Planning Target Volume (PTV). Boron concentrations in PTV, CTV and GTV were 10%, 50% and 100% respectively.

The neutron source uses a 30 MeV cyclotron. Neutrons are processed using Double Layer Beam Shaping Assembly (DLBSA). The energy spectrum of the neutrons produced by DLBSA is the thermal, epithermal, and fast neutrons, with epithermal neutrons dominating with an energy range of  $10^{-6}$  to  $10^{-2}$  MeV. The neutrons produced by DLBSA have a neutron flux characteristic of  $1.1 \times 10^9$  n/cm<sup>2</sup>.s, the ratio of epithermal neutron flux to thermal neutron flux of 344, the ratio of epithermal neutron flux to fast neutron flux of 85, the ratio of dose rate of fast neutrons to epithermal flux is  $1.09 \times 10^{-13}$  Gy.cm<sup>2</sup>, and the ratio of gamma dose rate to epithermal neutron flux is  $1.85 \times 10^{-13}$  Gy.cm<sup>2</sup> [15].

The Modeling of phantom and neutron sources from DLBSA is performed using Particle and Heavy Ions Transport code System (PHITS) version 3.2. To get low statistical errors, the simulation is carried out with  $10^7$  particle history. The cross-sectional library data used for neutrons dan photons are JENDL-4.0[12]. The PHITS code used in the simulation has been licensed by Japan Atomic Energy Agency (JAEA).

### 2.2 Calculation of Dose Rate

The calculated dose includes boron, gamma, proton, and neutron doses [16]. The dose calculation begins with determining the neutron flux using a tally track. The value of the neutron flux is then used to calculate the boron dose rate, gamma dose rate, and proton dose rate. The dose rate calculation uses equations 1, 2, and 3. The neutron dose rate, on the other hand, is calculated separately using tally deposits.

#### 2.2.1 Boron Dose Rate

The boron dose rate is obtained from the reaction of thermal neutrons with boron-10. The reaction produces alpha and lithium particles. The boron dose rate was determined using Equation 1 [17].

$$\dot{D}_{\text{boron}} = \frac{\phi N_{\text{B-tissue}} \sigma_B Q (1.6 \times 10^{-13}) \text{ J/MeV}}{1 \frac{\text{J/kg}}{\text{Gy}}} \quad (1)$$

with  $\dot{D}_{\text{boron}}$  is dose rate (Gy/s),  $\phi$  is thermal neutron flux (n.cm<sup>-2</sup>.s<sup>-1</sup>),  $N_{\text{B-tissue}}$  is the number of boron in 1 kg of tissue (atoms/kg),  $\sigma_B$  is microscopic absorption cross section (cm<sup>2</sup>), and Q is the energy of particles (MeV).

### 2.2.2 Proton Dose Rate

The proton dose rate results from thermal neutron capture with nitrogen-14, which gives carbon-14 and 0.66 MeV protons. The proton dose rate is determined using Equation [17].

$$\dot{D}_{proton} = \frac{\phi N_{N-tissue} \sigma_N Q (1.6 \times 10^{-13}) \text{ J/MeV}}{1 \frac{\text{J/kg}}{\text{Gy}}} \quad (2)$$

with  $\dot{D}_{proton}$  is dose rate (Gy/s),  $\phi$  is thermal neutron flux ( $\text{n.cm}^{-2}.\text{s}^{-1}$ ),  $N_{N-tissue}$  is the number of nitrogen in 1 kg of tissue (atoms/kg),  $\sigma_N$  is microscopic absorption cross section ( $\text{cm}^2$ ), and  $Q$  is the energy of particles (MeV).

### 2.2.3 Gamma Dose Rate

The reaction between thermal neutrons and hydrogens will produce gammas, having an energy of 2.33 MeV. The gamma dose rate is calculated by Equation 3.

$$\dot{D}_\gamma = \phi N_{H-tissue} \sigma_H \Delta \phi \quad (3)$$

with  $\phi$  is thermal neutron flux ( $\text{n.cm}^{-2}.\text{s}^{-1}$ ),  $N_{H-tissue}$  is the number of hydrogen atoms in 1 kg of tissue (atoms/kg), and  $\sigma_H$  is microscopic cross-section ( $\text{cm}^2$ ),  $\Delta$  is the coefficient of absorption dose rate, and  $\phi$  fractional dose rate of gamma [17].

### 2.3 Calculation of Total Dose Rate

The total dose rate is obtained by multiplying the absorbed dose by the radiation weight factor. The total dose rate is an equivalent dose, which corresponds to the level of damage to body tissues due to the absorption of some amount of radiation energy, taking into account the influencing factors. The total dose rate is calculated based on Equation 4 [18].

$$\dot{D}_{total} = W_b \times D_b + W_p \times D_p + W_n \times D_n + W_\gamma \times D_\gamma \quad (4)$$

With  $\dot{D}_{total}$  is the total dose rate,  $w_b$ ,  $w_p$ ,  $w_n$ , dan  $w_\gamma$  are radiation quality factors of boron, proton, neutron, and gamma, respectively. The radiation quality factors are shown in Table 1.

**Table 1** Radiation weight factors [19]

Symbol	Radiation Source	Radiation Weight Factor
$w_b$	Boron	3.8 (tumor)
		1.3 (healthy tissues)
$w_p$	Proton	3.2
$w_n$	Neutron	3.2
$w_\gamma$	Scattering	
	Gamma	1

### 2.4 Calculation of Radiation Time

The irradiation time is determined based on the minimum dose to kill cancer divided by the total dose. The dose to kill cancer is around 54 Gy [20]. Furthermore, the irradiation time is determined based on equation 5.

$$T = \frac{D_{min}}{D_{total}} \quad (5)$$

with  $T$  is irradiation time (s),  $D_{min}$  is the minimum tissue-damaging dose or the prescribed standard to kill cancer, and  $D_{total}$  is total dose rate absorbed by cancer cells (Gy/s).

## 3.0 RESULTS AND DISCUSSION

### 3.1 Neutron Irradiation on Neck Phantom

Figure 2 shows the interaction of the epithermal neutron radiation with the neck phantom. The neutron beam hits the neck organ mainly on the thyroid with different intensities. The intensity is highest at the surface (shown in yellow) and lowest at the back of the head (in blue). The change in intensity is caused by the neutron attenuation as it passes through tissues of different densities. The interaction of epithermal neutrons with tissues in the neck organs turns them into thermal neutrons [21].

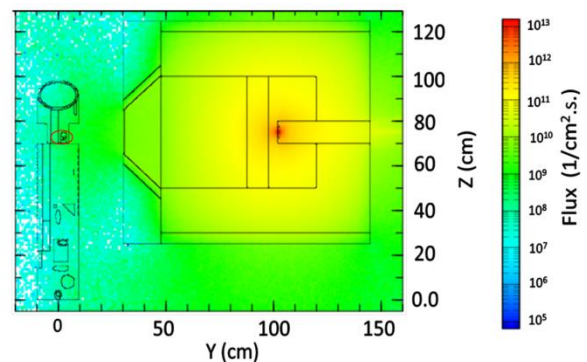


**Figure 2** Epithermal neutron interaction of a 30 MeV cyclotron-based DLBSA with the thyroid gland in the phantom neck (red circle mark)

The thermal neutron profile that penetrates the thyroid gland is shown in Figure 3. The figure shows that the thermal neutron flux at the depths of  $< 2$  cm increases and reaches a peak at the depths of 2-3 cm. Thermal neutron flux experiences a sharp decrease at 3 cm deep. The highest thermal neutron flux is obtained at a depth of 2.4 cm. The accumulation of thermal neutrons at a depth of 2.4 cm is due to the epithermal neutrons entering the neck tissue experiencing a lot of scattering, resulting in a decrease in energy and turning the epithermal

neutrons into thermal neutrons. Accumulation usually occurs at depths between 2-2.5 cm.

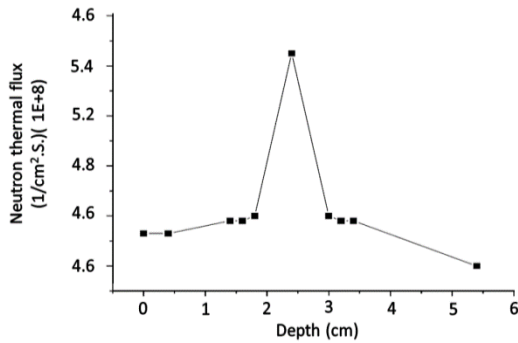


**Figure 3** Profile of thermal neutron flux penetrating the thyroid organ

### 3.2 Dose Rate

Figure 4 shows the dose rate components received by the neck organs using a boron concentration of 70 µg boron/g-tissue. The dose rate received by the organs in the neck has varying values. The highest dose value received by the cancer center was GTV with a dose rate of 3.036 x 10<sup>-3</sup> Gy/s. The high dose rate is due to GTV containing the most boron. The boron content in GTV is assumed to be 100%.

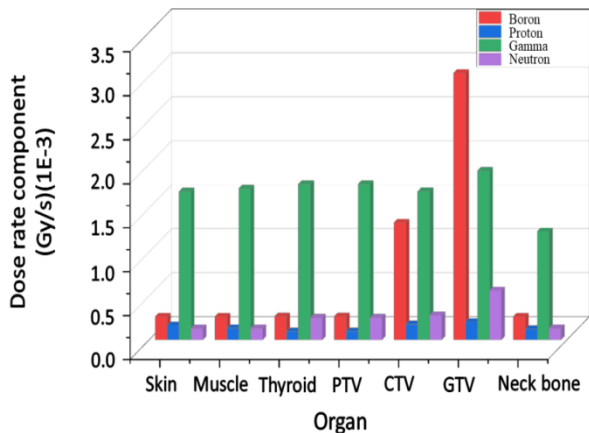


**Figure 4** The dose rate components in the neck organs: skin, muscle, thyroid, bone and cancer, calculated at a concentration of 70 g boron/g-tissue

The gamma dose rate in the neck phantom organs is greater than the proton and neutron dose rate. The value of the gamma dose rate in these organs produces uniform values except for the spine. The high rate of gamma dose is due to the same percentage of hydrogen in healthy and cancerous tissues, causing the thermal neutron interaction to produce a gamma dose rate with values that tend to be the same in these organs [22].

The lowest contribution to the dose rate comes from the proton dose rate, which is 2.031 x 10<sup>-4</sup> Gy/s. The proton dose rate results from thermal neutron capture with nitrogen-14, which gives carbon-14 and 0.66 MeV protons. The low value of the proton dose rate is due to low nitrogen content in the composition of elements that constitutes the body tissues (3%) [23]. The dose rate components on the neck organs, namely skin, muscle, toroid, bone, and cancer, calculated at a concentration of 70 µg boron/g-tissue, is shown in Figure 4.

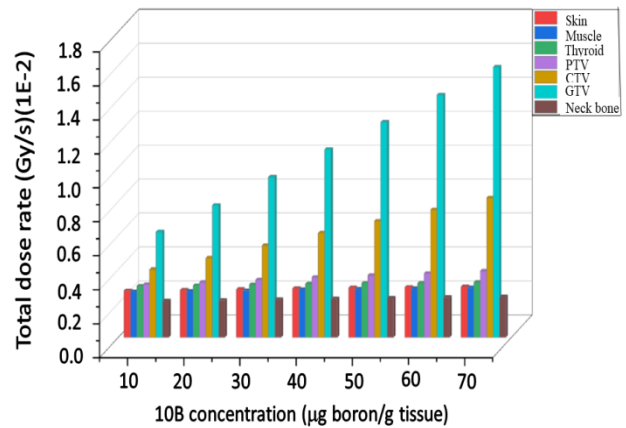


**Figure 5** The effect of concentration of <sup>10</sup>B on the total dose rate of neck organs

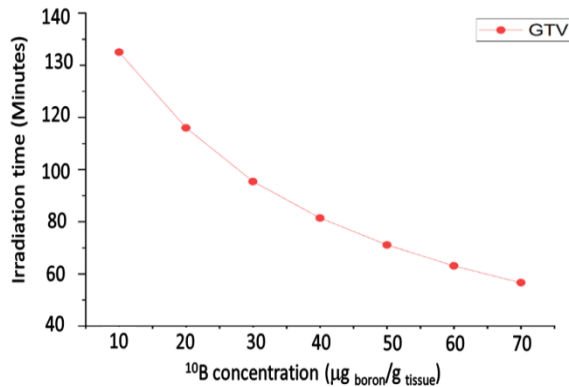
Figure 5 shows the effect of boron concentration on the total dose rate in neck organs. The figure shows that the increase in the concentration of <sup>10</sup>B causes the value of the total dose rate in cancer cells, consisting of PTV, CTV, and GTV, to increase. The highest total dose rate was received by GTV, with a total dose rate of 1.590 x 10<sup>-2</sup> Gy/s. The difference in the dose rate is caused by the difference in the content of <sup>10</sup>B in that section. The content of <sup>10</sup>B in PTV, CTV, and GTV is 10%, 50%, and 100%, respectively.

Figure 5 also shows that the lowest total dose rate is found at a concentration of 10 µg boron/g-tissue, with a total dose rate of 6.206 x 10<sup>-3</sup> Gy/s. The low boron content results in low interaction of thermal neutrons with boron. As a result, the dose rate is also low. The results obtained are in accordance with the results of research conducted by Ardana and Sardjono, (2017) which states that the dose rate is influenced by the concentration of <sup>10</sup>B [24].

Such a low total dose rate is also found in the skin, muscle, thyroid, and neck bone, which tends close to the dose rate value in PTV. Because healthy cells are assumed to contain 10% <sup>10</sup>B. The total dose rate is generated by the interaction of thermal neutrons with hydrogen atoms, interactions of thermal neutrons with nitrogen, and thermal neutron interactions with healthy cells containing 10% of <sup>10</sup>B. Consequently the total dose rate is lower than that of CTV and GTV.

### 3.2 Irradiation Time

The irradiation time can be obtained as the ratio of the minimum dose to kill cancer cells and the total dose rate of the BNCT components. The total dose rate is taken with reference to the GTV section, considering that GTV is a major part of cancer. The minimum dose to destroy cancer cells for thyroid cancer is 54 Gy [19, 24]. Hence, the irradiation time is obtained by dividing 54 Gy by the total dose rate in GTV. The results of the calculation of the irradiation time are shown in Figure 6.



**Figure 6** The effect of concentration on irradiation time

Figure 6 shows that the higher the concentration of  $^{10}\text{B}$ , the shorter the irradiation time needed for cancer therapy. The longest therapy time, which is 133 minutes, occurs at a concentration of 10  $\mu\text{g boron/g-tissue}$ , and the shortest time, which is 57 minutes, occurs at a concentration of 70  $\mu\text{g boron/g-tissue}$ . The irradiation time produced at a boron concentration of 70  $\mu\text{g boron/g-tissue}$  is the most effective therapeutic time for thyroid cancer therapy because the recommended time for BNCT therapy is less than one hour [24].

For 57 minutes, healthy tissues (skin) receive a dose rate of  $2.98 \times 10^{-3}$  Gy/s. The total dose received by the skin is 10.1 Gy. The value is below the allowed threshold for healthy cells, which is 12 Gy [24].

### 4.0 CONCLUSION

The radiation dose in thyroid cancer has been analyzed successfully using the PHITS Code. The neutron source is simulated using moderated epithermal neutrons using a 30 MeV cyclotron-based Double Layer Beam Shaping Assembly (DLBSA). The simulation results show that the epithermal neutron flux produced by DLBSA can penetrate the organs in the neck and transform themselves into thermal neutrons. The highest thermal neutron flux occurs at a depth of 2.4 cm. The results of the calculation of the dose rate components of boron, neutrons,

protons, and gamma in the skin, muscle, toroid, neck bone, and cancer organs at a concentration of 70  $\mu\text{g/g-tissue}$  show that the dose rate received by these organs varies. The highest dose rate components value received by the cancer center is in GTV, with a dose rate of  $3.036 \times 10^{-3}$  Gy/s. The results of the calculation of the total dose rate using concentrations of (10, 20, 30, 40, 50, 60, and 70)  $\mu\text{g/g-tissue}$ , show that the highest dose rate is at a concentration of 70  $\mu\text{g boron/g-tissue}$  with a dose rate of  $1,590 \times 10^{-2}$  Gy/s. According to the calculation, the best time for thyroid cancer therapy is at a boron concentration of 70  $\mu\text{g/g-tissue}$ , and the most effective treatment time is 57 minutes. During the irradiation time, healthy cells received a radiation dose below the allowed threshold.

### Conflicts of Interest

The author(s) declare(s) that there is no conflict of interest regarding the publication of this paper.

### Acknowledgement

The author expresses his gratitude to Institutions for Research and community service (LPPM) Jenderal Soedirman University which has fully funded this research through the 2023 Unsoed Basic Research Grant.

### References

- [1] Mullur, R., Liu, Y. Y., and Brent, G. A. 2014. Thyroid Hormone Regulation of Metabolism. *Physiological Reviews*. Doi: 10.1152/physrev.00030.2013
- [2] Beynon, M. E., and Pinneri, K. 2016. An Overview of the Thyroid Gland and Thyroid-related Deaths for the Forensic Pathologist. *Academic Forensic Pathology*. 6(2): 217-236. Doi: 10.23907/2016.024.
- [3] Takahashi, N., Matsushita, H., Umezawa, R., Yamamoto, T., Ishikawa, Y., Katagiri, Y., and Jingu, K. 2019. Hypofractionated Radiotherapy for Anaplastic Thyroid Carcinoma: 15 Years of Experience in a Single Institution. *European Thyroid Journal*. 8(1): 24-30. Doi: 10.1159/000493315.
- [4] Corrigan, K. L., Williamson, H., Elliott Range, D., Niedzwiecki, D., Brizel, D. M., and Mowery, Y. M. 2019. Treatment Outcomes in Anaplastic Thyroid Cancer. *Journal of Thyroid Research*. 1-11. Doi: 10.1155/2019/8218949.
- [5] Oktajianto, H., and Setiawati, E. 2016. Monte Carlo Simulation in Internal Radiotherapy of Thyroid Cancer. *Int J Eng Technol Manage Res*. 3(9): 16-24. Doi: <https://doi.org/10.29121/ijetmr.v5.i2.2018.669>.
- [6] Albano, D., Benenati, M., Bruno, A., Bruno, F., Calandri, M., Caruso, D., and Messina, C. 2021. Imaging Side Effects and Complications of Chemotherapy and Radiation Therapy: A Pictorial Review from Head to Toe. *Insights Into Imaging*. 12(1): 1-28. Doi: <https://doi.org/10.1186/s13244-021-01017-2>
- [7] Skwierawska, D., López-Valverde, J. A., Balcerzyk, M., and Leal, A. 2022. Clinical Viability of Boron Neutron Capture Therapy for Personalized Radiation Treatment. *Cancers*. 14(12): 2865.

- Doi: <https://doi.org/10.3390/cancers14122865>.
- [8] Moss, R. 2015. Critical Review with an Optimistic Outlook on Boron Neutron Capture Therapy (BNCT). *Applied Radiation and Isotopes*. 88: 2-11.  
Doi: [10.1016/j.apradiso.2013.11.109](https://doi.org/10.1016/j.apradiso.2013.11.109).
- [9] Tanaka, H., Takata, T., Watanabe, T., Suzuki, M., Mitsumoto, T., Kawabata, S., and Ono, K. 2020. Characteristic Evaluation of the Thermal Neutron Irradiation Field using a 30 MeV Cyclotron Accelerator for Basic Research on Neutron Capture Therapy. *Nuclear Instruments and Methods in Physics Research Section A: Accelerators, Spectrometers, Detectors and Associated Equipment*. 983: 164533.  
Doi: <https://doi.org/10.1016/j.nima.2020.164533>.
- [10] Li, G., Jiang, W., Zhang, L., Chen, W., and Li, Q. 2021. Design of Beam Shaping Assemblies for Accelerator-Based BNCT with Multi-Terminals. *Frontiers in Public Health*. 9.  
Doi: <https://doi.org/10.3389/fpubh.2021.642561>.
- [11] Faghghi, F., and Khalili, S. 2013. Beam Shaping Assembly of a D – T Neutron Source for BNCT and its Dosimetry Simulation in Deeply-seated Tumor. *Journal of Radiation Physics and Chemistry*. 89: 13-13.  
Doi: [10.1016/j.radphyschem.2013.02.003](https://doi.org/10.1016/j.radphyschem.2013.02.003).
- [12] Sato, T., Iwamoto, Y., Hashimoto, S., Ogawa, T., Furuta, T., Abe, S. I., and Niita, K. 2018. Features of Particle and Heavy Ion Transport Code System (PHITS) Version 3.02. *Journal of Nuclear Science and Technology*. 55(6): 684-690.  
Doi: <https://doi.org/10.1080/00223131.2017.1419890>.
- [13] Kumada, H., Takada, K., Aihara, T., Matsumura, A., Sakurai, H., and Sakae, T. 2020. Verification for Dose Estimation Performance of a Monte-Carlo based Treatment Planning System in University of Tsukuba. *Applied Radiation and Isotopes*. 166: 109222  
Doi: [10.1016/j.apradiso.2020.109222](https://doi.org/10.1016/j.apradiso.2020.109222).
- [14] Zankl, M., Becker, J., Lee, C., Bolch, W. E., Yeom, Y. S., and Kim, C. H. 2018. Computational Phantoms, ICRP/ICRU, and Further Developments. *Annals of the ICRP*. 47(3-4): 35-44.  
Doi: <https://doi.org/10.1177/0146645318756229>.
- [15] Bilalodin, B., Suparta, G. B., Hermanto, A., Palupi, D. S., and Sardjono, Y. 2019. Optimization and Analysis of Neutron Distribution on 30 MeV Cyclotron-based Double Layer Beam Shaping Assembly (DLBSA). *Nuclear Physics and Atomic Energy*. 20: 70-75.  
Doi: [10.15407/jnpae.2019.01.070](https://doi.org/10.15407/jnpae.2019.01.070).
- [16] Hu, N., Tanaka, H., Yoshikawa, S., Miyao, M., Akita, K., Aihara, T., and Ono, K. 2021. Development of a Dose Distribution Shifter to Fit Inside the Collimator of a Boron Neutron Capture Therapy Irradiation System to Treat Superficial Tumours. *Physica Medica*. 82: 17-24.  
Doi: <https://doi.org/10.1016/j.ejmp.2021.01.003>.
- [17] Harish, A. F., and Sardjono, Y. 2018. Dose Analysis of Boron Neutron Capture Therapy (BNCT) Treatment for Lung Cancer Based on Particle and Heavy Ion Transport Code System (PHITS). *ASEAN Journal on Science and Technology for Development*. 35(3): 187-194  
Doi: <https://doi.org/10.29037/ajstd.545>.
- [18] Pedrosa-Rivera, M., Praena, J., Porras, I., Ruiz-Magaña, M. J., and Ruiz-Ruiz, C. 2020. A Simple Approximation for the Evaluation of the Photon Iso-effective Dose in Boron Neutron Capture Therapy based on Dose-independent Weighting Factors. *Applied Radiation and Isotopes*. 157: 109018  
Doi: [10.1016/j.apradiso.2019.109018](https://doi.org/10.1016/j.apradiso.2019.109018).
- [19] Rasouli, and Masoudi. 2012. Design and Optimization of a Beam Shaping Assembly for BNCT based on D-T Neutron Generator and Dose Evaluation using a Simulated Head Phantom. *Applied Radiation Isotopes*. 70(12): 2755-2762.  
Doi: [10.1016/j.apradiso.2012.08.008](https://doi.org/10.1016/j.apradiso.2012.08.008).
- [20] Haugen, B. R., Alexander, E. K., Bible, K. C., Doherty, G. M., Mandel, S. J., Nikiforov, Y. E., ... & Wartofsky, L. 2016. American Thyroid Association Management Guidelines for Adult Patients with Thyroid Nodules and Differentiated Thyroid Cancer: The American Thyroid Association Guidelines Task Force on Thyroid Nodules and Differentiated Thyroid Cancer. *Thyroid*. 26(1): 1-133.  
Doi: [10.1089/thy.2015.0020](https://doi.org/10.1089/thy.2015.0020).
- [21] Bilalodin, Haryadi, A., Sari, K., Wihantoro. 2022. Optimization and Verification of Double Layer Beam Shaping Assembly (DLBSA) for Epithelial Neutron Generation. *Jurnal Teknologi*. 84(4): 103-112.  
Doi: <https://doi.org/10.11113/jurnalteknologi.v84.18047>.
- [22] Martin, J. E. 2006. *Physics for Radiation Protection*. 2nd ed. Weinheim: Wiley-Vch Verlag GmbH & Co.
- [23] Chellan, P., and Sadler, P. J. 2015. The Elements of Life and Medicines. *Philosophical Transactions of the Royal Society A: Mathematical, Physical and Engineering Sciences*. 373(2037): 20140182.  
Doi: <https://doi.org/10.1098/rsta.2014.0182>.
- [24] Ardana, I., and Sardjono, Y. 2017. Optimization of a Neutron Beam Shaping Assembly Design for BNCT and Its Dosimetry Simulation based on MCNPX. *Tri Dasa Mega*. 19(3): 121-130.  
Doi: <http://dx.doi.org/10.17146/tdm.2017.19.3.3582>.